Validation of a fast and sensitive UPLC-MS/MS quantitative method for *N*-acyl taurine analysis in biological samples

Gianna Falascina [a], Laure B. Bindels [b], Vincenzo Di Marzo [a,c], Adele Cutignano [a,*]

[a] *Consiglio Nazionale delle Ricerche (CNR), Istituto di Chimica Biomolecolare (ICB), Pozzuoli, NA, Italy*
[b] *Metabolism and Nutrition Research Group, Louvain Drug Research Institute, Université catholique de Louvain, UCLouvain, Brussels, Belgium*
[c] *Canada Excellence Research Chair on the Microbiome-Endocannabinoidome Axis in Metabolic Health, Institut Universitaire de Cardiologie et de Pneumologie de Québec and Institut sur la Nutrition et les Aliments Fonctionnels, Centre NUTRISS, Université Laval, Quebec City, Canada*

ABSTRACT

The recent discovery of *N*-acyl taurines (NATs) as a class of endogenous bioactive lipids and the perspective of their possible pharmacological applications stimulated the development of mass spectrometry-based methods for their quantitative measurements in biological tissues and fluids. We report here for the first time a procedure validated both in liver surrogate matrix and neat solvent (MeOH) based on UPLC-ESI-QqQ analysis for the identification and quantification of NATs in biological tissue extracts. The LC-MS method was based on five representative lipid analogues, including saturated, monounsaturated and polyunsaturated species, namely *N*-palmitoyl taurine (C16:0 NAT), *N*-oleoyl taurine (C18:1 NAT), *N*-arachidonoyl taurine (C20:4 NAT), *N*-docosanoyl taurine (C22:0 NAT) and *N*-nervonoyl taurine (C24:1 NAT), and evaluated for specificity, linearity, matrix effect, recovery, repeatability and intermediate precision and accuracy. The method validated in MeOH by internal standard approach (d$_4$-C20:4 NAT) showed excellent linearity in the range 1–300 ng/ml with R always $\geq$ 0.9996 for all NATs; intra-day and inter-day precision and accuracy were always within the acceptable range. Specificity was assessed on NAT standards in MeOH, applying the confirmation ratio of two diagnostic MRM ion transitions for product ions at *m/z* 80 and *m/z* 107 to true samples in the adopted BEH C18 UPLC conditions. Limit of detection (LOD) and limit of quantification (LOQ) were 0.3–0.4 and 1 ng/ml, respectively, for all compounds. The method was successfully applied to assess the levels of NATs in the mouse liver and, for the first time, in varying sections of the intestine (duodenum, jejunum, ileum and colon). NAT levels increased from duodenum to colon, evidencing a remarkable prevalence in the large intestine of C22:0 NAT, typically occurring mainly in the central nervous system. These findings prompt further studies to disclose the biological function of the various members of this class in different peripheral tissues.

1. Introduction

N-Acyl taurines (NATs) are a lipid class chemically constituted by a fatty acyl chain of various length (C16-C24) and number of double bonds covalently linked by amide-bond to the non-proteinogenic amino acid taurine, a primary bioactive amine with a terminal sulfonic acid group. They are described as being important members of the large family of endocannabinoid-like, or endocannabinoidome, mediators [1–4].

NATs were described for the first time in the mouse central nervous system as endogenous substrates of fatty acid amide hydrolase (FAAH) [5]. Later, they were reported in other mouse peripheral tissues,

including the liver and kidney, as well as in plasma as a variable pool of saturated and unsaturated fatty acid-derivatives, allowing to delineate a peculiar prevalence of long chain (C22 and C24) saturated fatty acid in the brain with respect to other shorter and/or polyunsaturated derivatives [6,7] in the liver and other tissues. More recently they were also described in human tissues, including also specific cell structures such as the islets of Langherans [8] and in plasma [9].

The identification of this new class of lipid mediators prompted soon after the search of their biological role and their possible involvement in human diseases. It has been described that NATs are ligands of the transient receptor potential (TRP) family of cation channels. In particular, the activation of TRPV1 and TRPV4 channels expressed in the
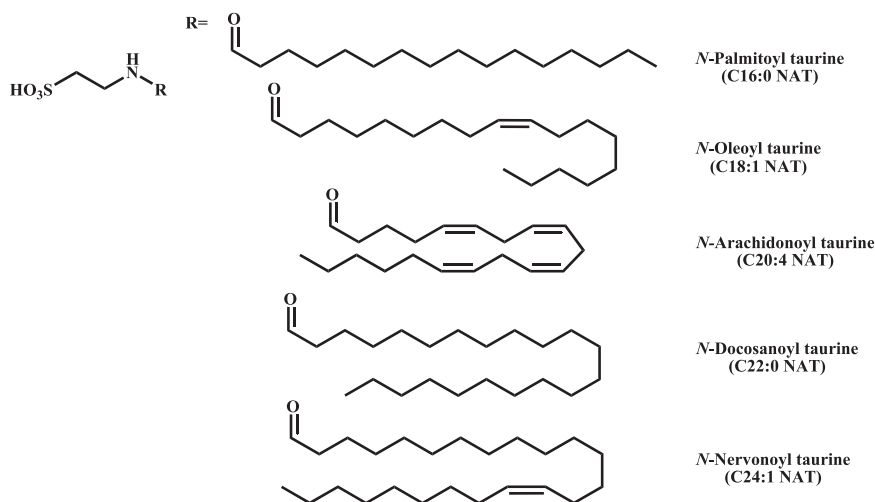

Fig. 1. Chemical structures of representative *N*-acyl taurines.

kidney suggested a possible involvement at the renal level in the regulation of blood pressure and osmotic balance [6,10]. TRP receptors may play a significant role in glucose homeostasis and indeed the treatment of mouse pancreatic β cells with *N*-oleoyl taurine (C18:1 NAT) and *N*-arachidonoyl taurine (C20:4 NAT) induced an increase in insulin release by activating the TRPV1 channels [11]. Furthermore, accumulation of these endogenous "lipoaminoacids" was observed in β-cells disfunction in vitro [8], while in vivo experiments in a mouse model showed that exogenous C18:1 NAT reduces food intake, improves insulin sensitivity and stimulates the secretion of glucagone-like peptide 1 (GLP-1) [9]. Interestingly, an analgesic action of C20:4 NAT due to inhibition of calcium channels of type T/ Cav3.2 in sensory neurons was also observed [12]. Reduced levels of two long-chain saturated NATs, i. e. *N*-eicosanoyl taurine (C20:0 NAT) and *N*-tetracosanoyl taurine (C24:0 NAT) were measured at the margins of a freshly inflicted wound to mouse skin, but they increased again as healing begins [13]. More recent is the discovery of the involvement of C20:4 NAT-induced activation of TRPV1 in the prefrontal cortex with protective effects on neurological disorders, similar to those of capsaicin [14]. Finally, very low concentrations (1 μM) of C20:4 NAT and C18:1 NAT have shown an anti-proliferative action on human prostate adenocarcinoma PC-3 cells [15].

The number of reports on the multiple biological processes involving NATs is rising although their biological functions in pathophysiological conditions are yet to be fully understood as well as their possible pharmacological applications. Hence, the availability of a validated, fast and sensitive method to specifically identify and quantify these molecules in biological tissues and fluids will be increasingly important. In the literature, different MS-based approaches have been proposed for NAT measurement [5–7,9,13,16] (Supplementary Material, Table S1). In all cases they rely on silica-based bonded phase columns eluted with either acidic or basic modifiers. However, no validated method has been published so far, nor any specific measurement has been carried out for the various NATs differing for length and unsaturation degree.

The aim of the present work was therefore to develop and validate a quantitative method based on ultraperformance liquid chromatography coupled to triple quadrupole-mass spectrometry for NAT analysis in biological tissues. In our study the UPLC-MS/MS quantitative method was validated by using five representative NATs covering the range C16-C24 of fatty acids and including saturated, monounsaturated and polyunsaturated species, namely *N*-palmitoyl taurine (C16:0 NAT), C18:1 NAT, C20:4 NAT, *N*-docosanoyl taurine (C22:0 NAT) and *N*-nervonoyl taurine (C24:1 NAT) (Fig. 1) and d4-C20:4 NAT as Internal Standard, and applied to assess the levels of these endogenous NATs in the mouse liver and for the first time, to the best of our knowledge, in the digestive tract (duodenum, jejunum, ileum and colon).

2. Materials and methods

2.1. Animal care and biological material

Male CD2F1 mice (7 weeks old, Charles River Laboratories, Italy) were housed in individually ventilated cages with a 12 h light/dark cycle and fed an irradiated chow diet (AO4–10, 2.9 kcal/g, Safe, France). After 22 days, mice were fasted for 5 h prior necropsy and euthanized by dislocation under anesthesia (isoflurane gas, Abbot, Belgium). Liver was collected and frozen in liquid nitrogen. Intestinal fragments were collected, rinsed in phosphate buffer solution and frozen in liquid nitrogen. All the samples were stored at − 80 °C until further analyses. The experiments were approved by and performed in accordance with the guidelines of the local ethics committee from the Université catholique de Louvain. Housing conditions were as specified by the Belgian Law of 29 May 2013, regarding the protection of laboratory animals (agreement no LA1230314).

2.2. Chemicals

HPLC grade Methanol (MeOH) and *tert*-Butyl methyl ether (MTBE) for sample extraction were purchased by VWR International (Milan, Italy); LC-MS hypergrade MeOH for LCMS analysis was from Merck (Merck KGaA, Darmstadt, Germany) as well as Ammonium hydroxide solution used as LCMS eluent modifier.

Ultrapure water was produced by a MilliQ apparatus (Millipore, Merck KGaA, Darmstadt, Germany). Reference standards (purity> 98 %) of C16:0 NAT, C18:1 NAT, C20:4 NAT, C22:0 NAT, and C24:1 and d4-C20:4 NAT were supplied by Cayman Chemical (Ann Arbor, Michigan, USA).

2.3. Standard solutions

Stock standard solutions (1 mg/ml) for each NAT were prepared in MeOH and stored at − 80 °C. For the construction of the calibration curves six calibration points were prepared by diluting working standard solutions (10 μg/ml) to obtain the final concentration of 1, 3, 10, 30, 100 and 300 ng/ml, spiked with 100 ng/ml of IS. QC samples were prepared at low, middle and high concentration levels (1, 3, 30 and 300 ng/ml).

2.4. NAT-free matrix preparation

A tissue homogenate was prepared from pooled mouse livers in PBS

buffer (pH 7.4) (Gibco, Thermo Fisher, Rodano, Italy) (1:8 w/v) on ice by using ULTRA-TURRAX T10 basic apparatus (IKA, Staufen, Germany) and incubated at 37 °C in orbital shaker (400 rpm) to allow FAAH enzyme to hydrolyze endogenous NATs. At time T = 0, 1, 2 and 4 hrs aliquots (50 μl) of homogenates were extracted in duplicate by using a MTBE/MeOH extraction protocol [17]. Briefly, cold MeOH (300 μl) and MTBE (1 ml) were added to the homogenate, mixed by vortex and sonicated. After 30 min, 250 μl of milliQ H_2O were added to each sample and after 10 min of shaking phase separation was induced by centrifugation at 10,000g for 10 min at 4 °C. The upper organic phase was carefully transferred to a glass vial. The aqueous phase was subjected to a second extraction by adding 300 μl of MTBE, shaking for 30 min and centrifuging as above. The organic extracts were combined, concentrated under a nitrogen stream and finally dried under vacuum. After 4 hrs of incubation the homogenate still showed a residual amount of most abundant endogenous NATs, hence it was diluted 1:10 for validation studies and frozen for successive analysis. Before validation in matrix, the homogenate was stabilized by adding the FAAH inhibitor URB597 (Merck, Milan, Italy) at a final concentration of 10 μM. The extracts were reconstituted in MeOH for LC-MS analysis.

2.5. Sample preparation

Frozen mouse tissues of liver (46–75 mg), duodenum (14–28 mg), jejunum (17–31 mg), ileum (4–19 mg) and colon (11–25 mg) (six biological replicates for each tissue) were quickly weighted in 2 ml Eppendorf tubes and directly extracted by using the MTBE/MeOH/H_2O biphasic extraction protocol reported above [17]. IS (10 μl of a 1 μg/ml solution in MeOH) was added to frozen tissues which were homogenized in organic solvent on ice. For ULPC-MS/MS analysis each extract was resuspended in 100 μl of MeOH (IS final concentration: 100 ng/ml).

2.6. LC-MS analysis

Chromatographic separations were achieved by a Waters (Milford, MA, USA) ACQUITY UPLC BEH C18 column (100 ×2.1 mm, 1.7 μm) at 60 °C on a Waters ACQUITY UPLC System. Eluent A: H_2O:MeOH (95:5, v/v) -ammonium hydroxide 0.1 % and eluent B: MeOH 100 %- ammonium hydroxide 0.1 %. The elution program consisted of an isocratic elution at 60 % eluent B for 1 min, followed by a gradient from 60 % to 95 % B in 4 min, holding 2 min at 95 %B, then returning at 60 % in 0.5 min; 2.5 min of a re-equilibration step was included in the program for a total elution time of 10 min. The flow was set at 0.3 ml/min. The injection volume was 2 μl. The autosampler was maintained at 10 °C. Weak needle wash solvent: H_2O:ACN (80:20); strong needle wash solvent: H_2O:ACN (25:75). NATs standards and IS were eluted at the following retention times: IS 2.88 min, C20:4 NAT 2.89 min, C16:0 NAT 3.11 min, C18:1 NAT 3.32 min, C22:0 NAT 4.66 min and C24:1 NAT 4.72 min

Mass spectrometry (MS) analysis was carried out by a MRM method developed on API 3200 Triple Quadrupole (ABSciex, Foster City, CA, USA) equipped with a Turbo V Ion Spray Source used in negative-ionization mode. Quantitation was achieved monitoring the $[M-H]^-$ ion at m/z 362.2 (C16:0 NAT), m/z 388.0 (C18:1 NAT), m/z 410.0 (C20:4 NAT), m/z 445.8 (C22:0 NAT) and m/z 472.1 (C24:1 NAT) in the first quadrupole and the product ions at m/z 80.0 (quantifier) and m/z 107.0 (qualifier) in the third quadrupole for each precursor ion. For IS, the transition of the precursor ion $[M-H]^-$ at m/z 414.0 > 80.0 was considered. The following source parameters were used: curtain gas at 20 psi, ion source gas (GS1) at 45 psi, turbogas (GS2) at 55 psi, desolvation temperature at 450 °C, collision gas (CAD) at 5 a.u. and ionspray voltage at − 4500 V. The collision energy (CE), declustering potential (DP), and entrance potential (EP) were optimized for each analyte and the internal standard by infusing the tuning solution (1 μg/ml) and were reported in Supporting Material Table S2. The dwell time was set to 50msec. The autosampler was maintained at 10 °C. Analyst

software (version 1.5.2; ABSciex) was used for data recording and Multiquant software (version 2.0.2; ABSciex) for quantitative analyses.

2.7. Method validation

The LC-MS/MS method was validated through evaluation of specificity, linearity, matrix effect, recovery, repeatability and intermediate precision and accuracy in accordance with the ICH Q2(R1) [18] and FDA [19] guidelines on validation of analytical procedures. Each analytical batch consisted of blank samples, zero samples, QC samples, calibration standards at different concentration levels (in MeOH or in liver matrix, with IS) and/or unknown samples.

2.7.1. Specificity

Two ion transitions (quantifier and qualifier) were monitored for each standard in MeOH solution. The ion transitions ratio was calculated for each NAT standard and together with the retention time these parameters were used as confirmation of NAT specific identification in biological samples excluding cross-reacting interfering molecules. Chromatographic and spectrometric parameters were optimized to minimize the interference on the analyte from endogenous substances and to obtain the highest signal to noise ratio (Supplementary Material, Table S2). No interfering compound was detected in blank samples of the surrogate matrix used for the validation.

2.7.2. Linearity

Six concentration levels of the five NATs standards in MeOH or in liver matrix (1, 3, 10, 30, 100, 300 ng/ml) were used (n = 4–6 replicates) to build up the calibration curve. A known amount of IS (100 ng/ml final concentration) was added at all calibration points. Peak area ratios of NAT standards/IS were used to express the analytical response *vs* NAT standard concentration (ng/ml). Limit of detection (LOD) was estimated by the calibration curve as $(3.3 * \sigma)/S$ where σ is the SD of y-intercepts and S is the slope of the curve. Limit of quantitation (LOQ) was defined as $(10 * \sigma)/S$. LOD and LOQ were both established in liver matrix and in MeOH.

2.7.3. Repeatability, intermediate precision and accuracy

Intra- and inter-day precision and accuracy were determined through the analysis of four-six replicates at four concentration levels (1, 3, 30 and 300 ng/ml) of NATs standards within the same day or over three consecutive days both in liver matrix and in MeOH. The samples were prepared according to the procedure mentioned before. The precision was expressed as coefficient of variation (CV, [standard deviation/measured mean concentration] * 100), while the accuracy was expressed as [measured mean concentration/nominal concentration] * 100.

2.7.4. Matrix effect

Aliquots of NAT-free liver homogenate were extracted as described above and spiked after extraction with known amounts (3, 30 and 300 ng) of the five NAT standards. The matrix effect (%) was evaluated comparing the response of each NAT spiked in the surrogate matrix post-extraction (Area$_{post}$) with that of NAT spiked in the solvent (Area$_{MeOH}$) as follows: (Area$_{post}$ -Area$_{MeOH}$)* 100/Area$_{MeOH}$. Results are expressed as a mean of six replicates.

2.7.5. Recovery

Aliquots of NAT-free liver homogenate were spiked before or after extraction with known amounts (3, 30 and 300 ng) of the five NAT standards. Recovery was calculated comparing the response of each NAT added to surrogate matrix before (Area$_{pre}$) and after extraction (Area$_{post}$) and expressed as follows: (Area$_{pre}$/Area$_{post}$)* 100. Results are means of six replicates.
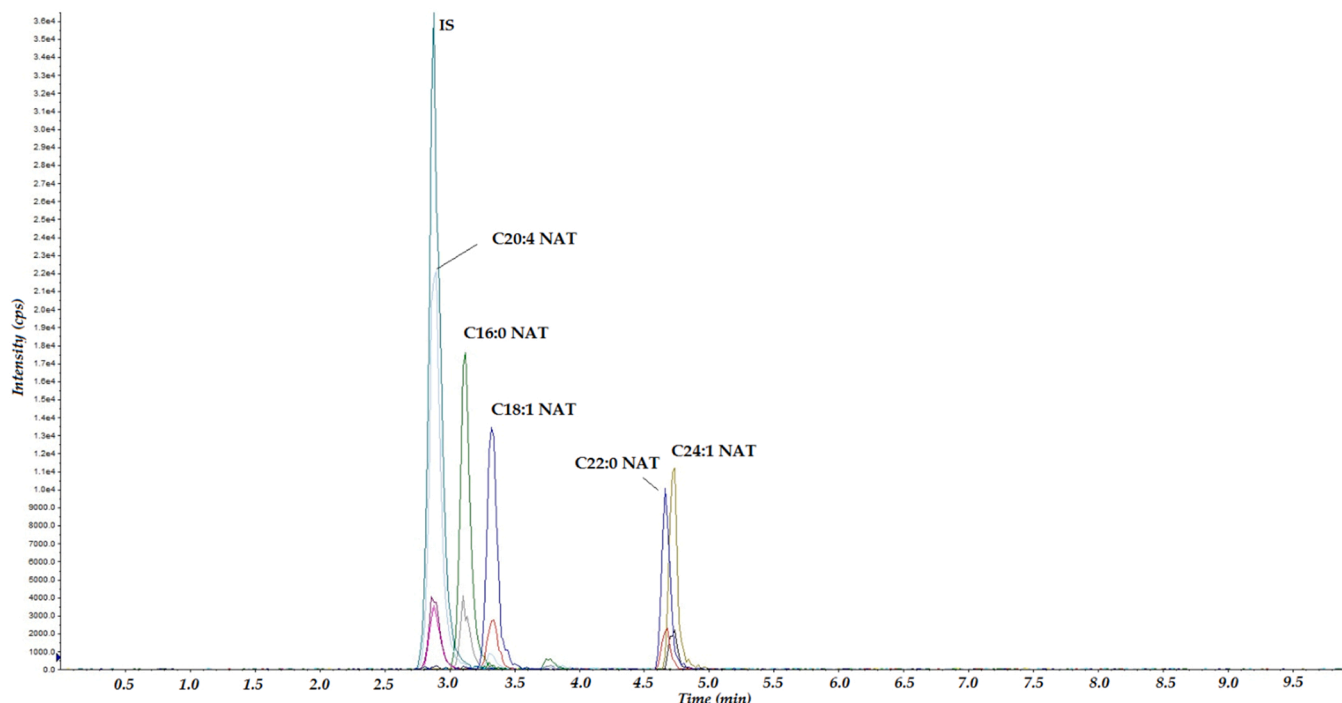
Fig. 2. Representative LC-MS chromatogram for NAT-standard mixture and IS (d_4-C20:4 NAT). Both quantifier (Precursor ion > Product ion *m/z* 80) and qualifier transitions (Precursor Ion > Product ion *m/z* 107) were shown for each compound.

2.7.6. Stability

Analyte stability studies were carried out at low, medium and high concentration levels (3, 30 and 300 ng/ml, respectively).

2.7.6.1. Bench-top stability. Extracted NAT-free matrix was spiked with the NAT standards and IS and left two hours at room temperature. Afterward, QCs were analyzed (n = 6) against freshly prepared calibration curves and QCs.

2.7.6.2. Autosampler stability. Extracted NAT-free matrix was spiked with the NAT standards and left 72 h in the autosampler at 10 °C. NAT level was assessed against freshly prepared calibration curves and QCs (n = 6).

2.7.6.3. Freeze-Thaw stability. Analyte stability in extracted spiked surrogate matrix was established after three freeze-thaw cycles with at least 12 h freezing, against freshly prepared calibration curves and QCs
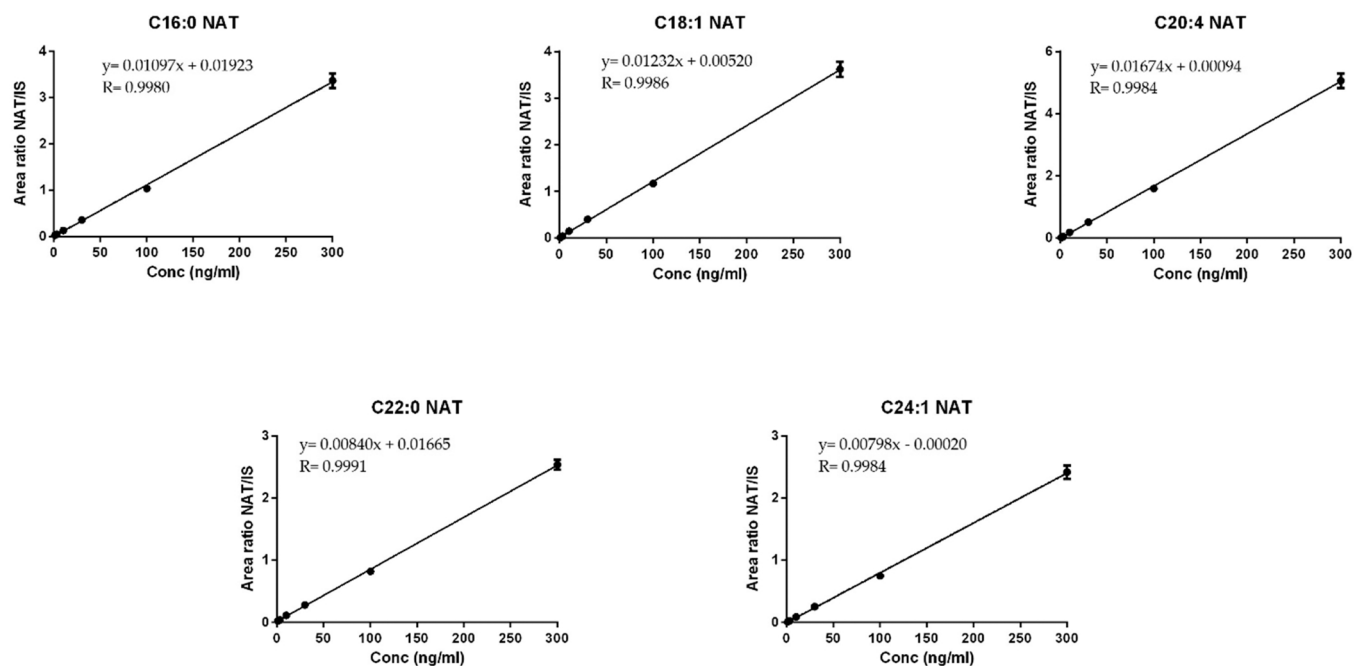

Fig. 3. Calibration curves in liver surrogate matrix for the LC-MS/MS analysis of the five NAT standards in the range 1–300 ng/ml. d_4-C20:4 NAT was used as IS (n = 6). Relative response (NAT peak area)/(IS peak area) vs NAT concentration (ng/ml). Corresponding linear regression equations (weighting=1/x) are reported above each graph.

Table 1

Intra-day and inter-day precision and accuracy, LOD and LOQ for the selected NATs by calibration curves in surrogate liver matrix.

		Intra-day[a] Nominal concentration (ng/ml)				Inter-day[b]				LOD	LOQ
		1	3	30	300	1	3	30	300		
C16:0 NAT	Precision (CV %)[c]	16.1	10.6	6.2	4.7	19.0	15.1	4.9	6.2	0.5	1.5
	Accuracy (%)[d]	100.2	94.1	104.3	101.7	103.7	97.8	100.5	101.0		
C18:1 NAT	Precision (CV %)	10.1	4.6	6.6	3.4	10.3	4.1	6.2	3.4	0.5	1.5
	Accuracy (%)	80.5	116.6	107.7	99.2	93.7	102.8	105.6	99.4		
C20:4 NAT	Precision (CV %)	13.0	4.7	5.2	4.8	11.0	7.6	6.3	4.6	0.5	1.5
	Accuracy (%)	90.2	97.9	104.3	100.7	89.3	105.0	103.6	100.1		
C22:0 NAT	Precision (CV %)	6.7	7.7	2.4	9.5	20.0	9.8	9.2	8.1	0.5	1.5
	Accuracy (%)	83.3	99.3	106.4	100.1	80.1	105.9	104.4	100.2		
C24:1 NAT	Precision (CV %)	8.6	6.5	5.8	4.3	14.0	13.3	5.3	4.6	0.5	1.5
	Accuracy (%)	86.4	102.1	106.6	101.0	89.2	99.6	106.2	99.9		

[a] n = 6 replicates.
[b] n = 6 replicates for 3 consecutive days.
[c] (Standard deviation/ measured mean concentration) * 100.
[d] (Measured mean concentration/ nominal concentration) * 100.

(n = 3).

3. Results and discussion

3.1. Method set-up and validation

Working solutions at a concentration of 1 μg/ml for each of the five NAT standards and for the IS d_4-C20:4 NAT were prepared in MeOH and infused in the mass spectrometer at 10 μl/min to optimize the MS parameters (Supporting Table S2). All [M-H]⁻ precursor ions of NATs fragmented at the taurine end to give as main products two ions at m/z 80.0 (SO₃) and 107.0 (CH₂ =CH-SO₃), which were selected as quantifier and qualifier transitions, respectively. The ratio (%) between these two transitions was measured for all lipid species and used as confirmation value to assess structural specificity in extracted samples (Supporting Table S2). The range measured varied from 15.5 to 23.6 and peak identification in the extract was considered acceptable with ± 15 % accuracy.

Starting from reported methods [5–7,9,13,16] summarized in Supplementary Table S1 and in order to obtain the best peak shape and resolution we tested several HPLC columns (Phenomenex Kinetex F5 and Luna NH₂, and Waters BEH C18), eluents (water and MeOH, isopropanol and/or acetonitrile), modifiers (acidic and basic buffers) and gradients, on our UPLC-Acquity system. Satisfactory results were finally obtained by using a BEH C18 column (100 ×2.1 mm, 1.7 μm) heated at 60 °C and an elution gradient of increasing MeOH in water, both containing 0.1 % Ammonium hydroxide to improve ionization in negative mode and peak shape, for a total run time of 10 min including a re-equilibration step. A representative chromatogram is reported in Fig. 2.

In absence of an analyte-free matrix, we attempted to prepare a surrogate matrix starting from mouse liver homogenates, as reported in Section 2.4. Calibration curves were constructed in the surrogate-matrix by using d_4-C20:4 NAT as the IS and the five representative NAT-

Table 3

Comparison of NAT levels (ng/ml) in mouse liver tissue by calibration curve of NAT/IS prepared in surrogate matrix and in MeOH.

	Matrix[a]	MeOH[a]	Difference %[b]
C16:0 NAT	26.2 ± 2.4	28.8 ± 2.7	9.9
C18:1 NAT	35.4 ± 5.4	37.5 ± 6.0	5.9
C20:4 NAT	13.4 ± 1.1	13.1 ± 1.2	2.2
C22:0 NAT	12.3 ± 2.1	12.0 ± 3.6	2.4
C24:1 NAT	5.9 ± 0.2	6.3 ± 0.9	6.8

[a] Values are reported as means of two biological replicates.
[b] (Measured mean concentration in MeOH- Measured mean concentration in matrix)* 100/Measured mean concentration in matrix.

standards and peak area ratios NAT/IS were plotted against concentration in the range 1–300 ng/ml. Linearity, intra-day and inter-day precision and accuracy, recovery and matrix effect were evaluated. The concentration-response best fitted a linear regression model (1/x) for all standard compounds with coefficients of correlation (R) ≥ 0.998 (Fig. 3 and Table 1).

Accuracy was reported as percent (%) at the four selected concentrations and was always 100 ± 15 % (± 20 % at the LOQ), accomplishing the criteria of acceptance indicated by the ICH Q2(R1) [18] and FDA [19] guidelines. Likewise, coefficients of variations (CV %) obtained for the intra-day and inter-day precision, respectively, were always below 15 % (≤20 % at the LOQ). Recoveries are typically high by using the MTBE/MeOH extraction protocol [17,20] and here never below 78 %; thus, the followed protocol resulted suitable for the extraction of low level lipids from liver and similar biological matrices (Table 2). Finally, the matrix effect (ME) was calculated by spiking NAT standards at three concentrations post-extraction in matrix and the peak areas compared to those measured for NAT spiked in MeOH: an ion enhancement was appreciated for all compounds (Table 2).

Probably the best way to avoid a ME is to resort to a matrix-matched/ standard addition calibration procedure. However, this approach is
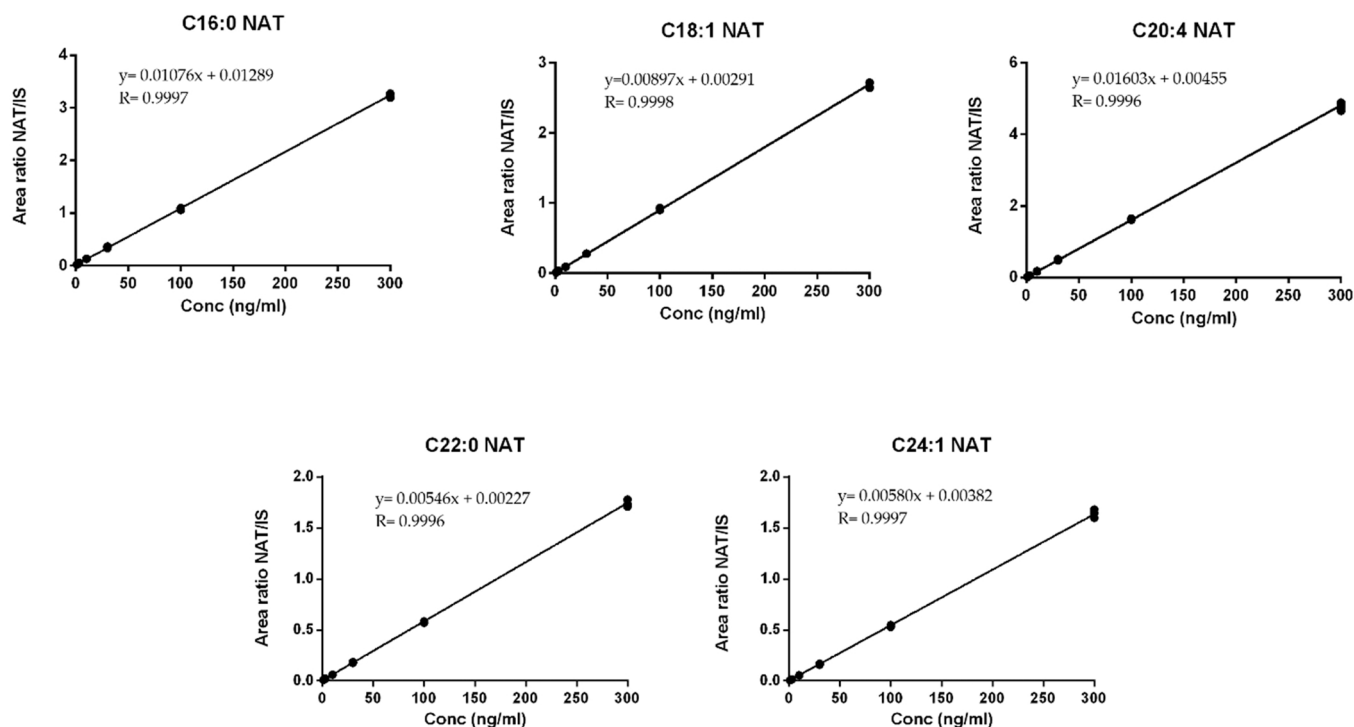
Table 2

Matrix Effect and Recovery for the selected NATs.

	Matrix Effect (ME)[a] Nominal concentration (ng/ml)			IS-normalized ME			Recovery[b]		
	3	30	300	3	30	300	3	30	300
C16:0 NAT	24.3	19.3	40.2	4.6	4.3	2.6	88.1	81.8	80.0
C18:1 NAT	14.0	24.4	32.8	2.6	5.4	2.1	88.7	82.8	80.4
C20:4 NAT	16.2	20.4	27.8	3.1	4.5	1.8	80.9	79.0	83.8
C22:0 NAT	26.8	28.3	46.7	5.1	6.3	3.0	97.2	83.3	78.0
C24:1 NAT	39.4	23.0	47.2	7.5	5.1	3.1	89.6	91.8	86.5

Values are mean concentrations of six replicates [a](Area_post-Area_MeOH) * 100/A_MeOH; [b] (Area_pre/Area_post) * 100.

Fig. 4. Calibration curves for the LC-MS/MS analysis of the five NAT standards in the range 1–300 ng/ml. d_4-C20:4 NAT was used as internal standard (n = 4). Relative response (NAT peak area)/(IS peak area) vs NAT concentration (ng/ml). Corresponding linear regression equations (weighting=1/x) are reported above each graph.

Table 4
Intra-day and inter-day precision and accuracy, LOD and LOQ for the selected NATs by calibration curves in MeOH.

		Intra-day[a] Nominal concentration (ng/ml)				Inter-day[b]				LOD	LOQ
		1	3	30	300	1	3	30	300		
C16:0 NAT	Precision (CV %)[c]	12.7	1.0	4.3	1.3	13.7	14.7	11.0	9.1	0.4	1.1
	Accuracy (%)[d]	81.4	106.5	103.9	99.4	80.1	112.8	106.6	100.0		
C18:1 NAT	Precision (CV %)	8.8	5.3	1.6	1.6	13.6	12.3	13.6	13.3	0.3	1.0
	Accuracy (%)	89.1	103.8	102.7	99.0	86.6	108.68	103.4	99.8		
C20:4 NAT	Precision (CV %)	8.0	2.6	3.0	2.4	9.0	9.2	7.7	4.7	0.4	1.1
	Accuracy (%)	84.3	104.6	103.3	99.2	86.4	106.6	105.7	99.8		
C22:0 NAT	Precision (CV %)	6.1	7.32	3.74	2.5	20.0	11.3	13.82	11.15	0.4	1.1
	Accuracy (%)	81.9	99.7	99.1	99.9	87.3	100.7	106.3	100.8		
C24:1 NAT	Precision (CV %)	6.0	11.4	2.0	2.0	19.8	14.6	9.1	6.9	0.3	1.1
	Accuracy (%)	92.8	113.3	102.6	99.8	94.7	107.8	102.8	99.4		

[a] n = 4 replicates.

[b] n = 4 replicates for 3 consecutive days.

[c] [Standard deviation/ measured mean concentration] × 100.

[d] [Measured mean concentration/ nominal concentration] × 100.

generally impractical since it requires large amounts of tissues that are not available for all biological models; indeed, here the use of an IS was adopted since the beginning to compensate for all analytical bias including a possible ME; in fact, when normalized for the IS-ME, the effective ME was totally acceptable for all NATs (Table 2). Considering the difficulties in preparing a NAT-free matrix we aimed at addressing the quantitative analysis of these lipids using MeOH, which as a neat solvent can be considered the simplest surrogate matrix. Hence, we performed a comparative measurement of the selected NATs in two mouse liver samples extracted by MTBE/MeOH adding the IS before extraction, using calibration curves freshly prepared in NAT-free matrix and in MeOH (Table 3).

As reported in Table 3, the values obtained were comparable and the difference between mean concentration values obtained in MeOH and those obtained in the surrogate matrix, was within 10 %. With this result

in our hands we validated the quantitative method in MeOH for linearity, intra-day and inter-day precision and accuracy, LOD and LOQ (Fig. 4 and Table 4). In this solvent, as well as previously in matrix, we found excellent parameters, thus the method resulted sensitive, precise and accurate.

Hence, we considered for further applications the use of MeOH as the simplest surrogate matrix suitable for the specific quantitation of NATs in biological tissues.

Finally, analyte stability was evaluated to ensure that every step taken during sample preparation and sample analysis, as well as the storage conditions used do not affect the concentration of the analytes. In particular, bench-top, autosampler (rack), and freeze-thaw stability were assessed (Supplementary Material, Table S3). Overall, we found no significant reduction in signal responses of measured QC concentration with respect to freshly prepared QCs and the observed variation (<15 %)
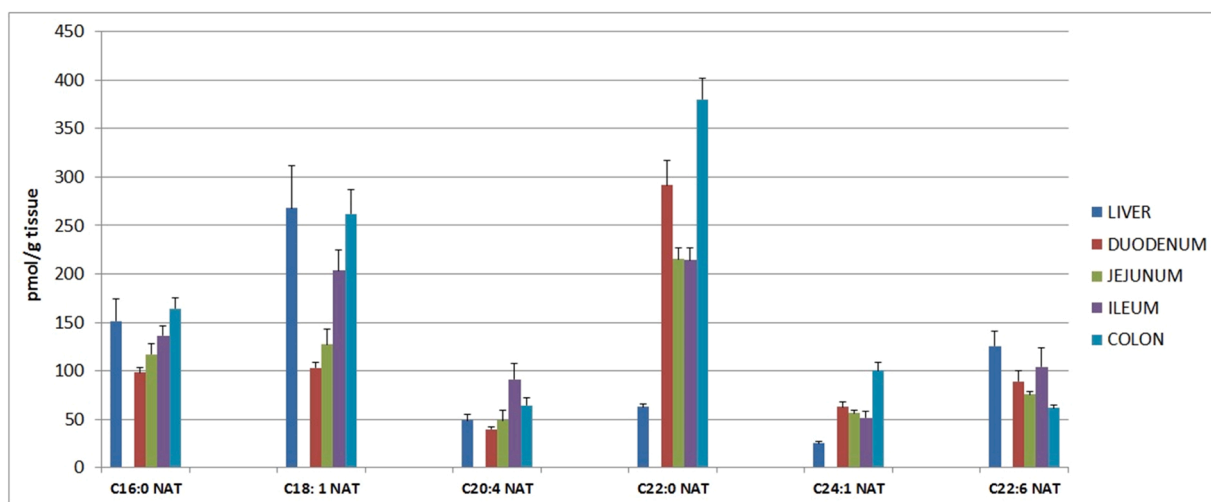
Fig. 5. Tissue levels for selected NATs expressed as pmol/g ± SEM (n = 6).

falls within the accuracy of the validated method. Therefore, NATs can be considered stable under the tested conditions.

3.2. Method Application to the quantitative analysis of representative NATs in the mouse liver and intestine tissues

Although most papers focus on changes in NAT levels, absolute quantification of individual NATs in specific tissues appear in same cases discordant probably even due to the lack of a specific method of quantification (Supplementary Table S1). The validated method here proposed was first applied to measure the level of the five selected NATs in liver. As reported in Fig. 5 and in Supplementary Fig. S1, long-chain saturated and monosaturated NATs such as C22:0 NAT and C24:1 NAT, typically abundant in brain tissues, are poorly represented in liver (25–50 pmol/g). This aspect has been previously disclosed [5–7] and the levels of these lipids are comparable with those already reported (9–20 pmol/g liver). On the other hand, the composition of polyunsaturated derivatives seems to be quite variable [6,7] although a predominance of *N*-docosahexaenoyl taurine (C22:6 NAT) above C20:4 NAT has been reported, generally attested on 20–34 pmol/g, in line with our finding (63 pmol/g). Hence, we attempted to use the calibration curve built-up to profile C20:4 NAT, structurally the closest species to C22:6 NAT. This latter lipid was putatively identified by using the instrumental settings optimized for C20:4 NAT and monitoring the two diagnostic MRM transitions common to all derivatives. Specifically, the two transitions at m/z 434 > 80 and m/z 434 > 107 gave rise to two peaks at Rt= 2.87 min with an area ratio of 16.7; this value was in the range measured for all the other standard NATs, strongly supporting the peak assignment to the C22:6 NAT (Supplementary Material, Table S2). Although this represented an approximation, effectively the levels estimated for C22:6 NAT were higher than C20:4 NAT and were attested around 125 pmol/g (Fig. 5). On the other hand, the levels of C16:0 NAT and C18:1 NAT we measured by using the corresponding NAT standards were higher than those reported in the literature, likely due to a less sensitive response for these compounds with consequent higher error while using i.e. quantitative calibration curves built on standards with different unsaturation degree or by using a single point calibration approach. However, a biological variability cannot be excluded.

To the best of our knowledge, no report has been published so far on the endogenous levels of NATs in the intestine. We compared the levels of the selected NATs as well as the putative C22:6 NAT in 4 dissected traits, i.e. duodenum, jejunum, ileum and colon. A progressive increase of C16:0 NAT and C18:1 NAT was observed moving from the small (duodenum, jejunum and ileum) to the large intestine (colon). While the levels of polyunsaturated species seem to be comparable among the

various intestinal sections and the liver, the most striking differences was ascribable to long-chain NATs that indeed are typically recovered in nervous system. In particular, C22:0 NAT was the most abundant lipid with very high levels (> 350 pmol/g) in the colon, suggesting that the exploration of the composition of these lipid species and the investigation of their biological function, in particular in the gastrointestinal system, deserve further studies.

4. Conclusions

A procedure validation for NAT measurement in biological tissues was reported here. An Internal Standard approach was used to set up a quantitative LC-MS/MS method developed on a UPLC-triple quadrupole platform. The method has been validated both in a surrogate NAT-depleted liver matrix and in MeOH and resulted suitable for specificity, accuracy, intra-day and inter-day precision, linearity, and recovery in a concentration range from 1 to 300 ng/ml. The lower limit of quantitation of the analytical method was 1 ng/ml for all tested NATs. This corresponds approximately to 2–3 pmol/g tissue weight, which means that down to 20 fmol can be easily measured in tissue samples weighing 10 mg. Indeed, the developed method was successfully applied to assess amounts of representative NATs in the mouse liver and for the first time in dissected sections of the intestine (duodenum, jejunum, ileum and colon), evidencing appreciable differences. In particular, long-chain NAT species, such as C22:0 NAT, generally reported as typically occurring mainly in central nervous system, showed remarkable abundance particularly in the colon above all the analyzed segments. These findings prompt further studies to understand in depth the regulation of NAT levels and define the NAT profile in the gastrointestinal tract, thus contributing to disclose the biological function of the various members of this class of lipid mediators in this and other peripheral tissues.

CRediT authorship contribution statement

Adele Cutignano: Conceptualization, Methodology, Formal analysis, Validation, Writing – original draft, Supervision, Investigation, Data analysis, Resources, Visualization, Writing – review & editing, Project administration. **Gianna Falascina:** Investigation, Data analysis, Visualization, Writing – review & editing. **Laure B. Bindels:** Investigation, Resources, Writing – review & editing. **Vincenzo Di Marzo:** Data analysis, Resources, Writing – review & editing, Funding acquisition.

Declaration of Competing Interest

The authors declare that they have no known competing financial interests or personal relationships that could have appeared to influence the work reported in this paper.

Acknowledgments

Appendix A. Supporting information

Supplementary data associated with this article can be found in the online version at doi:10.1016/j.jpba.2023.115252.

References

[1] F. Piscitelli, G. Carta, T. Bisogno, E. Murru, L. Cordeddu, K. Berge, S. Tandy, J. Cohn, M. Griinari, S. Banni, V. Di Marzo, Effect of dietary krill oil supplementation on the endocannabinoidome of metabolically relevant tissues from high-fat-fed mice, Nutr. Metab. 8 (2011) 1–16, https://doi.org/10.1186/1743-7075-8-51.

[2] V.Di Marzo, The endocannabinoidome as a substrate for noneuphoric phytocannabinoid action and gut microbiome dysfunction in neuropsychiatric disorders, Dialog. Clin. Neurosci. 22 (2020) 259–269, https://doi.org/10.31887/DCNS.2020.22.3/VDIMARZO.

[3] G. Morris, K. Walder, S. Kloiber, P. Amminger, M. Berk, C.C. Bortolasci, M. Maes, B. K. Puri, A.F. Carvalho, The endocannabinoidome in neuropsychiatry: opportunities and potential risks, Pharmacol. Res. 170 (2021), 105729, https://doi.org/10.1016/j.phrs.2021.105729.

[4] J. Lian, I. Casari, M. Falasca, Modulatory role of the endocannabinoidome in the pathophysiology of the gastrointestinal tract, Pharmacol. Res. 175 (2022), 106025, https://doi.org/10.1016/j.phrs.2021.106025.

[5] A. Saghatelian, S.A. Trauger, E.J. Want, E.G. Hawkins, G. Siuzdak, B.F. Cravatt, Assignment of endogenous substrates to enzymes by global metabolite profiling, Biochemistry 43 (2004) 14332–14339, https://doi.org/10.1021/bi0480335.

[6] A. Saghatelian, M.K. McKinney, M. Bandell, A. Patapoutian, B.F. Cravatt, A FAAH-regulated class of N-acyl taurines that activates TRP ion channels, Biochemistry 45 (2006) 9007–9015, https://doi.org/10.1021/bi0608008.

[7] J.Z. Long, M. LaCava, X. Jin, B.F. Cravatt, An anatomical and temporal portrait of physiological substrates for fatty acid amide hydrolase, J. Lipid Res. 52 (2011) 337–344, https://doi.org/10.1194/jlr.M012153.

[8] M. Aichler, D. Borgmann, J. Krumsiek, A. Buck, P.E. MacDonald, J.E.M. Fox, J. Lyon, P.E. Light, S. Keipert, M. Jastroch, A. Feuchtinger, N.S. Mueller, N. Sun, A. Palmer, T. Alexandrov, M. Hrabe de Angelis, S. Neschen, M.H. Tschöp, A. Walch, N-acyl taurines and acylcarnitines cause an imbalance in insulin synthesis and secretion provoking β cell dysfunction in Type 2 diabetes, Cell Metab. 25 (2017) 1334–1347.e4, https://doi.org/10.1016/j.cmet.2017.04.012.

[9] T.J. Grevengoed, S.A.J. Trammell, M.K. McKinney, N. Petersen, R.L. Cardone, J. S. Svenningsen, D. Ogasawara, C.C. Nexøe-Larsen, F.K. Knop, T.W. Schwartz, R. G. Kibbey, B.F. Cravatt, M.P. Gillum, N-acyl taurines are endogenous lipid messengers that improve glucose homeostasis, Proc. Natl. Acad. Sci. USA 116 (2019) 24770–24778, https://doi.org/10.1073/pnas.1916288116.

[10] M.K. McKinney, B.F. Gravatt, Structure-based design of a FAAH variant that discriminates between the N-acyl ethanolamine and taurine families of signaling lipids, Biochemistry 45 (2006) 9016–9022, https://doi.org/10.1021/bi0608010.

[11] D.P. Waluk, K. Vielfort, S. Derakhshan, H. Aro, M.C. Hunt, N-Acyl taurines trigger insulin secretion by increasing calcium flux in pancreatic β-cells, Biochem. Biophys. Res. Commun. 430 (2013) 54–59, https://doi.org/10.1016/j.bbrc.2012.11.026.

[12] G. Barbara, A. Alloui, J. Nargeot, P. Lory, A. Eschalier, E. Bourinet, J. Chemin, T-type calcium channel inhibition underlies the analgesic effects of the endogenous lipoamino acids, J. Neurosci. 29 (2009) 13106–13114, https://doi.org/10.1523/JNEUROSCI.2919-09.2009.

[13] O. Sasso, S. Pontis, A. Armirotti, G. Cardinali, D. Kovacs, M. Migliore, M. Summa, G. Moreno-Sanz, M. Picardo, D. Piomelli, Endogenous N- Acyl taurines regulate skin wound healing, Proc. Natl. Acad. Sci. USA 113 (2016) E4397–E4406, https://doi.org/10.1073/pnas.1605578113.

[14] M. Zhang, D. Ruwe, R. Saffari, M. Kravchenko, W. Zhang, Effects of TRPV1 activation by capsaicin and endogenous N-arachidonoyl taurine on synaptic transmission in the prefrontal cortex, Front. Neurosci. 14 (2020), https://doi.org/10.3389/fnins.2020.00091.

[15] V. Chatzakos, K. Slätis, T. Djureinovic, T. Helleday, M.C. Hunt, N-acyl taurines are anti-proliferative in prostate cancer cells, Lipids 47 (2012) 355–361, https://doi.org/10.1007/s11745-011-3639-9.

[16] M. Alhouayek, P. Bottemanne, K.V. Subramanian, D.M. Lambert, A. Makriyannis, P.D. Cani, G.G. Muccioli, N-acylethanolamine-hydrolyzing acid amidase inhibition increases colon N-palmitoylethanolamine levels and counteracts murine colitis, FASEB J. 29 (2015) 650–661, https://doi.org/10.1096/FJ.14-255208/-/DC1.

[17] V. Matyash, G. Liebisch, T.V. Kurzchalia, A. Shevchenko, D. Schwudke, Lipid extraction by methyl-terf-butyl ether for high-throughput lipidomics, J. Lipid Res. 49 (2008) 1137–1146, https://doi.org/10.1194/jlr.D700041-JLR200.

[18] ICH, Guideline Q2(R2) on validation of analytical procedures, 2, 2022.

[19] FDA, Bioanalytical method validation guidance for industry, Bioanal. Method Valid. (2018) 1–44.

[20] A. Cutignano, E. Luongo, G. Nuzzo, D. Pagano, E. Manzo, A. Sardo, A. Fontana, Profiling of complex lipids in marine microalgae by UHPLC/tandem mass spectrometry, Algal Res. 17 (2016) 348–358, https://doi.org/10.1016/j.algal.2016.05.016.